

Is the new model better? One metric says yes, but the other says no. Which metric do I use?

Qian M. Zhou^{a,1,2}, Zhe Lu^b, Russell J. Brooke^c, Melissa M Hudson^c, Yan Yuan^{b,2}

^a Department of Mathematics and Statistics, Mississippi State University,
Starkville, Mississippi 39762, USA

^b School of Public Health, University of Alberta,
Edmonton, AB T6G1C9, Canada

^c St Jude Children's Research Hospital, Memphis, TN 38105, USA

Abstract

Background: Incremental value (IncV) evaluates the performance change from an existing risk model to a new model. It is one of the key considerations in deciding whether a new risk model performs better than the existing one. Problems arise when different IncV metrics contradict each other. For example, compared with a prescribed-dose model, an ovarian-dose model for predicting acute ovarian failure has a slightly lower area under the receiver operating characteristic curve (AUC) but increases the area under the precision-recall curve (AP) by 48%. This phenomenon of conflicting conclusions is not uncommon, and it creates a dilemma in medical decision making.

Methods: In this article, we examine the analytical connections and differences between two IncV metrics: IncV in AUC (ΔAUC) and IncV in AP (ΔAP). Additionally, since they are both semi-proper scoring rules, we compare them with a strictly proper scoring rule: the IncV of the scaled Brier score (ΔsBrS), via a numerical study

Results: We demonstrate that both ΔAUC and ΔAP are weighted averages of the changes (from the existing model to the new one) in separating the risk score distributions between events and non-events. However, ΔAP assigns heavier weights to the changes in the high-risk group, whereas ΔAUC weights the changes equally. In the numerical study, we find that ΔAP has a wide range, from negative to positive, but the size of ΔAUC is much smaller. In addition, ΔAP and ΔsBrS are highly consistent, but ΔAUC is negatively correlated with ΔsBrS and ΔAP at a low event rate. ΔAUC and ΔAP are the least consistent among the three pairs, and their differences are more pronounced as the event rate decreases.

Conclusions: Choosing which metric to evaluate the IncV of a new model depends on the purpose of the prediction. If the risk model is used to identify the high-risk group, ΔAP is more appropriate, especially for a low event rate.

Keywords: High-risk group identification; Prediction performance; Brier score; Proper scoring rules; Rare outcome

1 Introduction

Risk prediction is crucial in many medical decision-making settings, such as managing disease prognosis. Numerous research has been dedicated to continually updating risk models for better prediction accuracy. For example, several papers have investigated the improvement in predicting the risk of cardiovascular disease by adding new biomarkers to the existing Framingham risk model, such as the C-reactive protein (Cook et al., 2006; Buckley et al., 2009), and more recently, a polygenic risk score (Mosley et al., 2020; Elliott et al., 2020).

In some applications, an existing marker is replaced with a new marker that provides more precise information. For example, cancer treatment such as radiation can have significant long-term health consequences for cancer survivors. Prescribed radiation doses to body regions, such as the abdomen and chest, are routinely available in medical charts. But to predict the risk of an organ-specific outcome, e.g., secondary lung cancer or ovarian failure, a more precise measurement of the radiation exposure to specific organs provides better information. Radiation oncologists developed and applied algorithms to estimate these organ-specific exposures (Howell et al., 2019).

The measurement of a new marker or the more precise measurement of a known risk factor is often costly and time-consuming. Thus, it is important to verify that the new model indeed has a measurable and better prediction performance than the existing one, and thus, worth the extra resources. A number of metrics have been proposed to evaluate the incremental value (IncV) of the risk model that incorporates the new information. The IncV has primarily been discussed in settings where new markers are added to the existing risk profile (Pencina et al., 2008; Pepe et al., 2013). In this paper, the term IncV refers to the change of the prediction performance whenever an existing risk model is compared with a new one.

In medical research, the receiver operating characteristic (ROC) curve has been the most popular tool for model evaluation, dating back to the 1960s when it was applied in diagnostic radiology and imaging systems (Zweig and Campbell, 1993; Pepe, 2003). The area under the ROC curve (AUC) captures the discriminatory ability of a model, i.e., how well a model separates events (subjects who experience the event of interest) from non-events (subjects who are event-free). Recently, the precision-recall (PR) curve is gaining popularity (Badawi et al., 2018; Chaudhury et al., 2019; Tang et al., 2019; Xiao et al., 2019). Originated from the information retrieval community in the 1980s (Raghavan et al., 1989; Manning and Schütze, 1999), it is a relatively new tool in medical research. The area under the PR curve is called the average positive predicted value or the average precision (AP) (Yuan et al., 2015; Su et al., 2015; Yuan et al., 2018). The AP evaluates the *prospective* prediction performance of a risk model because it is conditional on the risk score obtained at baseline. In contrast, the AUC is a *retrospective* metric that is conditional on future disease outcomes, unknown at baseline.

¹Dr. Zhou is the corresponding author.

Problems arise when the IncV in AUC and IncV in AP contradict each other, which is not uncommon. For example, a prescribed-dose model and an ovarian-dose model were compared in Clark et al. (2020) for predicting acute ovarian failure among female childhood cancer survivors. The ovarian-dose has a slightly lower AUC but an increased AP by about 48%, compared to the prescribed-dose model. Our numerical study results further demonstrate that the IncV in AUC and the IncV in AP do not agree in various scenarios when neither of the two competing working risk models is the true model. The disagreement creates confusion in decision making. In this article, we present explanations via unveiling their analytical relation and differences.

2 Notation, Definitions, and Data example

First, we lay out the notations and define concepts that are used throughout this article. Let $D = 0$ or 1 denote a binary outcome. For studies with an event time T , define $D = I(T \leq \tau)$ for a given prediction time period τ , which indicates that the outcome is time-dependent. In this article, we refer to subjects with $D = 1$ as the *events* and those with $D = 0$ as the *non-events*. Let $\pi = Pr(D = 1)$ denote the event rate.

2.1 Risk model and risk score

A risk model is a function of a set of predictors $\mathbf{X} = (\mathbf{X}_1, \dots, \mathbf{X}_{k-1})$, which might include interaction terms and polynomial terms, to obtain the probability of $D = 1$. Usually, we write this model as a regression model:

$$p(\mathbf{X}) = \mathbf{g}(\beta_0 + \beta_1 \mathbf{X}_1 + \dots + \beta_{k-1} \mathbf{X}_{k-1}), \quad (1)$$

where $g(\cdot)$ is a smooth and monotonic *link* function, such as a logit link. For the censored event time outcomes, a risk model could be Cox's proportional hazards model (Cox et al., 1972) or the time-specific generalized linear model (Uno et al., 2007); both models can be expressed in the general form of equation (1) with modifications.

In practice, the underlying data generating mechanism is often complicated, and our working risk model in equation (1) is usually misspecified. Let $\pi(\mathbf{X}) = \mathbf{Pr}(\mathbf{D} = \mathbf{1} \mid \mathbf{X})$ denote the *true* probability of $D = 1$, which is determined by the underlying distribution of D given \mathbf{X} . Here, we refer to $\pi(\mathbf{X})$ as the *true* risk and $p(\mathbf{X})$ as the *working* risk from a working risk model. When the working risk model in equation (1) is misspecified, $p(\mathbf{X}) \neq \pi(\mathbf{X})$.

The working risk $p(\mathbf{X})$ can be regarded as a risk score and used to classify subjects into different risk categories. For example, given a cut-off value c , subjects with $p(\mathbf{X}) \leq c$ are classified into the low-risk group, whereas the high-risk group consists of subjects with $p(\mathbf{X}) > c$. In general, a risk score, denoted as $r(\mathbf{X})$, can be any function of \mathbf{X} that reflects how likely a subject is an event. Thus, $r(\mathbf{X})$ can be a non-decreasing transformation of $p(\mathbf{X})$, e.g., $r(\mathbf{X}) = \mathbf{g}^{-1}(p(\mathbf{X})) = \beta_0 + \beta_1 \mathbf{X}_1 + \dots + \beta_{k-1} \mathbf{X}_{k-1}$.

Remark 1. In practice, the working risk $p(\mathbf{X})$ is estimated from a data sample. The estimated regression coefficients $\hat{\beta}_j$, $j = 0, 1, \dots, k-1$, are the solution to an estimating equation: $\Psi(\beta_0, \dots, \beta_{k-1}) = \sum_{i=1}^n \Psi(\beta_0, \dots, \beta_{k-1}; D_i, \mathbf{X}_i)$. The estimated risk given \mathbf{X} is $\hat{p}(\mathbf{X}) =$

$\mathbf{g}(\hat{\beta}_0 + \hat{\beta}_1 \mathbf{X}_1 + \dots + \hat{\beta}_{k-1} \mathbf{X}_{k-1})$, which is not of interest here. In this article, we investigate the predictive performance of the **population** working risk $p(\mathbf{X}) = \mathbf{g}(\beta_0^* + \beta_1^* \mathbf{X}_1 + \dots + \beta_{k-1}^* \mathbf{X}_{k-1})$ where β_j^* 's are the solution of $E_{(D, \mathbf{X})} [\Psi(\beta_0, \dots, \beta_{k-1})] = 0$ with the expectation taken under the true joint distribution of (D, \mathbf{X}) , and $\beta_j^* = \lim_{n \rightarrow \infty} \hat{\beta}_j$.

2.2 Accuracy measures and IncV metrics

The AUC and AP can be defined on any risk score $r(\mathbf{X})$ since they are rank-based. The ROC curve is a curve of the true positive rate (TPR) versus the false positive rate (FPR). Given a cut-off value c , the TPR and FPR are the proportions of higher risk $r(\mathbf{X}) > c$ among the events and non-events respectively, i.e., $\text{TPR}(c) = \Pr[r(\mathbf{X}) > c \mid \mathbf{D} = 1]$ and $\text{FPR}(c) = \Pr[r(\mathbf{X}) > c \mid \mathbf{D} = 0]$. The AUC can be interpreted as the conditional probability that given a pair of an event and a non-event, the event is assigned with a higher risk score, i.e., $\text{AUC} = \Pr[r(\mathbf{X}_i) > r(\mathbf{X}_j) \mid \mathbf{D}_i = 1, \mathbf{D}_j = 0]$.

The PR curve is a curve of the positive predicted value (PPV) versus the TPR. The PPV is defined as $\text{PPV}(c) = \Pr[D = 1 \mid r(\mathbf{X}) > c]$, the proportion of subjects with higher risk scores that are events. The AP can be expressed as $\text{AP} = E[\text{PPV}(r_1(\mathbf{X}))]$ (Yuan et al., 2018), where $r_1(\mathbf{X})$ denotes the risk score of an event, and the expectation is taken under the distribution of $r_1(\mathbf{X})$.

Both the AUC and AP are proper scoring rules: the true model has the maximum AUC and AP among all the models. One of their differences is that the AP is event-rate dependent (Yuan et al., 2018), whereas the AUC does not depend on π since it is conditional on the event status.

Let Ψ_{old} and Ψ_{new} denote an accuracy measure Ψ (e.g., AUC or AP) of the existing and new risk models, respectively. The IncV parameter is defined as $\Delta\Psi = \Psi_{new} - \Psi_{old}$, which quantifies the change in Ψ when comparing the new model with the existing one.

2.3 A data example

Accurate ovarian failure (AOF) is a complication from acute toxicity of exposure to radiation and chemotherapy. It is defined as permanent loss of ovarian function within 5 years of a cancer diagnosis or no menarche after cancer treatment by age 18. About 6% of female childhood cancer survivors have AOF. We evaluate and compare two recently published risk models (Clark et al., 2020) that predict AOF on an external validation dataset, the St. Jude Lifetime Cohort (Hudson et al., 2011), which consists of 875 survivors with 50 AOF events.

Both models include the following risk factors: age at cancer diagnosis, cumulative dose of alkylating drugs measured using the cyclophosphamide-equivalent dose, haematopoietic stem-cell transplant, and radiation exposure. The difference between the two models is in the measurement of radiation exposure. The *prescribed-dose* model uses the prescribed radiation doses to the abdominal and pelvic regions, which are routinely available in medical charts. The *ovarian-dose* model uses the minimum of the organ-specific radiation exposure for both ovaries estimated by radiation oncologists. The equation for calculating the AOF risk using each model is given in the supplementary material of Clark et al. (2020).

Figure 1 (a) shows the ROC curves and PR curves of these two models. The estimated AUC is 0.96 for the prescribed-dose model and 0.94 for the ovarian-dose model; ΔAUC is

estimated to be -0.02 . The estimated AP is 0.46 for the prescribed-dose model and 0.68 for the ovarian-dose model. The estimated ΔAP is 0.22. The estimation procedure is explained in Appendix.

Based on the IncV in AUC, we conclude that the ovarian-dose model is slightly worse than the prescribed-dose model, and as a result, there is no need to obtain the more expensive ovary dosimetry. However, based on the IncV in AP, the ovarian-dose model clearly outperforms the prescribed-dose model. Why do these two metrics give conflicting conclusions?

3 AUC and AP: Measuring the separation of the risk scores between events and non-events

To answer this question, we first investigate the connections and differences between the AUC and AP using the following three hypothetical risk scores: r_1 , r_2 , and r_3 . We assume that all the risk scores among non-events follow a standard normal distribution, i.e., $r_j | D = 0 \sim N(0, 1)$, for $j = 1, 2, 3$. However, their distributions among events are different: (i) $r_1 | D = 1 \sim N(1.8, 2)$, (ii) $r_2 | D = 1 \sim N(1.5, 1.5)$, and (iii) $r_3 | D = 1 \sim N(3, 1.5)$.

Figure 2 presents the comparisons of these three risk scores under an event rate $\pi = 0.05$. Figure 2 (a) shows their density curves stratified by events and non-events. Among them, the two density curves of r_3 are the most separated. Thus, the ROC and PR curves of r_3 dominate those of r_1 and r_2 (Figure 2 (b)), and consequently, r_3 has the largest AUC and AP. In contrast, the ROC and PR curves of r_1 and r_2 cross: r_2 has a slightly larger AUC with $\text{AUC}_{r_2} - \text{AUC}_{r_1} = 0.007$, but r_1 has a considerably larger AP with $\text{AP}_{r_1} - \text{AP}_{r_2} = 0.096$. Figure 3 exhibits the comparisons between r_1 and r_2 for three different event rates $\pi = 0.2$, 0.05, and 0.01.

Analytically, both the AUC and AP measure the separation of the risk score distributions between events and non-events. Let $F_1(\cdot)$ and $F_0(\cdot)$ denote the cumulative distribution functions (CDFs) of a risk score $r(\mathbf{X})$ conditional on $D = 1$ (events) and $D = 0$ (non-events), respectively. Let $q_\alpha = F_1^{-1}(\alpha)$ denote the α -th quantile for the distribution F_1 , $0 \leq \alpha \leq 1$. As shown in equations (A.4) and (A.5) of Appendix, the AUC and AP can be expressed as functions of $F_0(q_\alpha)$, the proportion of non-events whose risk scores are below the α -th quantile of the risk scores among events. The $F_0(q_\alpha)$ measures the separation of the two distributions F_1 and F_0 : the larger the $F_0(q_\alpha)$ is at a given α , the more non-events having lower risk scores, indicating a further separation between these two distributions. For example, the $F_0(q_\alpha)$ curve of r_3 dominates those of r_1 and r_2 (Figure 2 (b)), which is consistent with the fact that r_3 has the best separation between events and non-events (Figure 2 (a)).

Furthermore, we can express ΔAUC and ΔAP as

$$\Delta\Psi = \int_0^1 w_\Psi(\alpha) \Delta(\alpha) d\alpha, \quad \Psi = \text{AUC or AP}, \quad (2)$$

where $w_\Psi(\alpha)$ is a weight function, and $\Delta(\alpha) = F_{\text{new},0}(q_{\text{new},\alpha}) - F_{\text{old},0}(q_{\text{old},\alpha})$, capturing how much the new working risk model changes the separation of these two distributions at a

given α . Note that $\Delta(\alpha)$ is independent of π because it is conditional on the event outcome. Thus, ΔAUC and ΔAP are weighted averages of $\Delta(\alpha)$, but their weights are different. For ΔAUC , $w_{\text{AUC}}(\alpha) \equiv 1$ for $0 \leq \alpha \leq 1$, i.e., $\Delta(\alpha)$ is *equally* weighted. For ΔAP , $w_{\text{AP}}(\alpha)$ is a function of α and π (equation (A.6) of Appendix).

To visualize how $w_{\text{AP}}(\alpha)$ changes with α and π , we plot the $w_{\text{AP}}(\alpha)$ in a log scale against α for different π in Figure 3 (a), in the context of comparing the hypothetical risk scores r_1 and r_2 . For any π , $w_{\text{AP}}(\alpha)$ increases with α . This tells us that ΔAP assigns heavier weights to the upper-tail quantiles of the risk score, representing the higher-risk group, and lighter weights to the lower-tail quantiles, representing the lower-risk group, i.e., ΔAP emphasizes the change of the separation in the high-risk group. However, the change is equally weighted in ΔAUC since $w_{\text{AUC}}(\alpha) \equiv 1$.

Thus, when the main objective is to identify the high-risk group for intervention, such as when screening for a rare outcome, ΔAP is more appropriate than ΔAUC . On the other hand, for some classification problems, such as classifying early-stage or late-stage cancer, both the low-risk group and high-risk group may be of interest, and ΔAUC serves this purpose better.

Additionally, w_{AP} is affected by π . When π is smaller, $w_{\text{AP}}(\alpha)$ is larger for α values close to 1 but smaller for α values close to 0. This indicates that, at a lower event rate, if a risk model can better separate the two risk score distributions at the upper quantiles, it will be rewarded more; if it has a worse separation at the lower quantiles, it will be penalized less.

3.1 Hypothetic risk scores r_1 and r_2 revisited

Assuming that r_2 is from an existing risk model and r_1 is from a new one, $\Delta(\alpha) = F_{r_1,0}(q_{r_1,\alpha}) - F_{r_2,0}(q_{r_2,\alpha})$, $\Delta\text{AUC} = \text{AUC}_{r_1} - \text{AUC}_{r_2}$, and $\Delta\text{AP} = \text{AP}_{r_1} - \text{AP}_{r_2}$. As shown in Figure 3 (b), $\Delta(\alpha) > 0$ for large α , and $\Delta(\alpha) < 0$ for small α . It indicates that compared to r_2 , r_1 has a better separation for the upper quantiles of the risk score but worse for the lower quantiles. With equal weighting, ΔAUC is equivalent to the area under $\Delta(\alpha)$ curve over its entire range. Since the area above 0 is approximately the same as the area below 0, $\Delta\text{AUC} \approx 0$. As mentioned earlier, ΔAUC is invariant for different π . Thus, $\Delta\text{AUC} = -0.007$ (Figure 2 (b)) for all three π values.

For ΔAP , the r_1 's upper-tail better performance is weighted more than its lower-tail worse performance, which explains ΔAP is all positive for the three π values (Figure 3 (c)). Additionally, when π gets smaller, the better separation of r_1 at the upper quantiles is rewarded more, and meanwhile, its worse separation at the lower quantiles is penalized less. Thus, even though $\Delta(\alpha)$ stays the same across different π , ΔAP increases as π decreases (Figure 3 (c)).

3.2 Data example revisited

Let $\Delta(\alpha) = F_{\text{ovarian},0}(q_{\text{ovarian},\alpha}) - F_{\text{prescribed},0}(q_{\text{prescribed},\alpha})$. Figure 1 (b) plots the estimated $\Delta(\alpha)$, $w_{\text{AP}}(\alpha)$, and $w_{\text{AP}}(\alpha)\Delta(\alpha)$. It shows that the estimated $\Delta(\alpha) > 0$ for $\alpha > 10\%$, whereas the prescribed-dose model performs better with the estimated $\Delta(\alpha) < 0$ when $\alpha < 10\%$. It suggests that compared to the prescribed-dose model, the ovarian-dose model separates the events and non-events better among individuals predicted to be at a higher risk. Overall,

under the estimated $\Delta(\alpha)$ curve, the area below zero is slightly larger than the area above zero. Thus, the estimated ΔAUC is negative but close to zero. This indicates that these two models have comparable performance in terms of discrimination.

However, the estimated ΔAP rewards the superior performance of the ovarian-dose model at the upper quantiles with large weights, and thus, it is positive and sizable. Clark et al. (2020) created four risk groups: low ($< 5\%$), medium-low (5% to $< 20\%$), medium (20% to $< 50\%$), and high risk ($\geq 50\%$). The ovarian-dose model classifies 37 individuals (out of 875) as high risk, among which 30 (81%) experienced AOF, while the prescribed-dose model predicted 13 individuals at high risk, with 6 (46%) having developed AOF. This again confirms that the ovarian-dose model is better at identifying high-risk individuals.

Comparison with Brier score. Since both the AUC and AP are rank-based, they are semi-proper scoring rules: a misspecified working risk model and the true model can have the same AUC and AP when they rank the subjects' risks in the same order. We decide to compare these two metrics with the Brier score (BrS), the only strictly proper scoring rule.

The BrS is the expected squared difference between the binary outcome D and the working risk $p(\mathbf{X})$, i.e., $\text{BrS} = E_{(D, \mathbf{X})} \{[D - p(\mathbf{X})]^2\}$. The BrS is minimized at the true model, i.e., $p(\mathbf{X}) = \pi(\mathbf{X})$. A non-informative model, assigning the event rate to every subject, i.e., $p(\mathbf{X}) \equiv \pi$, leads to the maximum BrS value $\pi(1 - \pi)$. A *scaled Brier score* (sBrS) is defined as $\text{sBrS} = 1 - \text{BrS}/[\pi(1 - \pi)]$, ranging from 0 and 1, with larger values indicating better performance (Steyerberg et al., 2010).

Remark 2. Although the BrS cannot be directly expressed as a function of $F_0(q_\alpha)$, it is closely related to the two distributions F_1 and F_0 . Specifically, it can be written as

$$\text{BrS} = E \{[1 - p(\mathbf{X})]^2 \mid D = 1\} \pi + E \{[p(\mathbf{X})]^2 \mid D = 0\} (1 - \pi).$$

The first expectation is the mean squared prediction error (MSPE) of the working risk $p(\mathbf{X})$ for events, determined by the distribution F_1 , whereas the second expectation is the MSPE for non-events, determined by the distribution F_0 . Both MSPEs can be expressed as the sum of the variance of $p(\mathbf{X})$ and its squared bias from 1 for events and 0 for non-events. A smaller BrS can result from one, or a combination, of the following: (i) the mean of $p(\mathbf{X})$ for events closer to 1, (ii) the mean of $p(\mathbf{X})$ for non-events closer to 0, (iii) less variation in $p(\mathbf{X})$ for events or non-events or both. All of these lead to a further separation of the two distributions: F_1 and F_0 .

Let ΔsBrS denoted the IncV in sBrS. The sBrS is estimated to be 0.23 for the prescribed-dose model and 0.50 for the ovarian-dose model, and ΔsBrS is estimated to be 0.27. Thus, similar to ΔAP , ΔsBrS favors the ovarian-dose model.

Why are ΔsBrS and ΔAP consistent in this example? Figure S1 of the supplementary material shows the histogram of the predicted risk \hat{p}_i from each model among the AOF and non-AOF individuals. For the non-AOF individuals, the risk score distributions of these two models are similar. Consequently, the mean and variance of \hat{p}_i for both models are also similar: the mean is 0.033 for the ovarian-dose model and 0.042 for the prescribed-dose model; their variances are both about 0.0053. The MSPE for the ovarian-dose model is 0.0064, slightly lower than 0.0071 for the prescribed-dose model.

For the AOF events, the risk score distribution of the ovarian model has a heavier right tail. This indicates that the ovarian-dose model pushes more AOF events to the high-risk group. As a result, the mean of \hat{p}_i for the ovarian-dose model is 0.48, much closer to 1 than 0.23 for the prescribed-dose model. The variance is 0.10 for the ovarian dose model and 0.023 for the prescribed-dose model. The MSPE of the ovarian-dose model is 0.367, much smaller than 0.613 of the prescribed-dose model. Combining the MSPEs for events and non-events weighted by their respective proportions, the estimated BrS for the ovarian-dose model is 0.027, which is smaller than 0.042, the estimated BrS for the prescribed-dose model.

This data example illustrates a comparison of the three IncV parameters: ΔAUC , ΔAP , and ΔsBrS . Next, we expand the comparison via a numerical study.

4 Numerical Study

As we are interested in the IncV parameters of the population working risk, not in the IncV estimates from a sample, we do not use simulation studies. In this section, we conduct a numerical study to evaluate the IncV of adding a marker, denoted by Y , to a model with an existing marker, denoted by X . The IncV parameters can be directly derived from the distributional assumptions described below.

4.1 Setting

Let the markers X and Y be independent standard normal random variables. Given the values of these two markers, a binary outcome D follows a Bernoulli distribution with the probability of $D = 1$ via the following model:

$$\pi(X, Y) = \text{Pr}(D = 1 \mid X, Y) = \Phi(\beta_0 + \beta_1 X + \beta_2 Y + \beta_3 XY), \quad (3)$$

where $\Phi(\cdot)$ is the CDF of a standard normal distribution. Given X and Y , $\pi(X, Y)$ is the *true* risk. The true model in equation (3) includes an interaction between X and Y , indicating the effect of X on the risk changes with the value of Y , and vice versa.

Typically, in practice, none of the working models are the true model. Having this in mind, we compare the following two misspecified working models: (i) *one-marker model*: $p(X) = \Phi(\gamma_0 + \gamma_1 X)$, and (ii) *two-marker model*: $p(X, Y) = \Phi(\gamma_0 + \gamma_1 X + \gamma_2 Y)$.

Here, we consider different values of β_1 , β_2 , β_3 and π : $\beta_1 = 0.3, 0.4, \dots, 0.9, 1$, $\beta_2 = 0.3, 0.4, \dots, 0.9, 1$, $\beta_3 = -0.5, -0.4, \dots, -0.1, 0.1, \dots, 0.4, 0.5$ (excluding 0), and $\pi = 0.01, 0.05, 0.1, 0.2, 0.5$. Each combination of $(\beta_1, \beta_2, \beta_3, \pi)$ values is referred to as a scenario. Given a scenario, the value of β_0 can be derived. In the supplementary material, we explain how to obtain the value of β_0 and calculate the AUC, AP, and sBrS of the one-marker and two-marker models as well as the IncV parameter.

4.2 Results

We compare the three IncV parameters based on key considerations for a desirable IncV: (1) size and range, and (2) agreement. A desirable IncV metric should be sensitive to the change in the predictive performance. If a new model improves the prediction accuracy, an

IncV should have a sizable positive value. It should also be able to reflect a performance deterioration with a sizable negative value. If an IncV is often close to 0, we might question its utility in decision-making. We are also interested in the agreement among the three IncV parameters, given that they focus on different aspects of the prediction performance.

4.2.1 Size and Range

Figure 4 plots the summary statistics (minimum, 25% quantile, median, 75% quantile, and maximum) of the three IncV metrics under different event rates. ΔAP has the widest range, followed by $\Delta sBrS$, and ΔAUC has the narrowest range. This difference between ΔAUC and ΔAP is more evident for a lower event rate. For example, under $\pi = 0.01$, the inter-quartile range (IQR) and median of ΔAUC are both 0.07. In contrast, the IQR of ΔAP is much wider, with a range of about 0.41 and a median of 0.21.

In addition, ΔAUC is negative in less than 1% of the scenarios (29 out of 3200). Furthermore, when it is negative, the value is very close to 0, which indicates that ΔAUC cannot distinguish between a useless marker and a harmful marker (Kattan and Gerds, 2018). On the other hand, ΔAP is negative in about 12% of the scenarios (389 out of 3200), with a much larger size.

As π changes, the range of ΔAP varies the most among the three IncV metrics, whereas the quartiles of ΔAUC remain almost constant. As π increases, the ranges of all the IncV metrics get narrower and closer to each other. When $\pi = 0.5$, both ΔAUC and ΔAP range from 0.015 to 0.25 with a median of 0.089, and $\Delta sBrS$ ranges from 0.019 to 0.32 with a median of 0.12.

4.2.2 Agreement

Correlation. We calculate the Pearson correlation between each pair of the IncV metrics under each π (Table 1). ΔAP and $\Delta sBrS$ are highly correlated for all values of π . As π increases, their correlation decreases from about 1 ($\pi = 0.01$) to 0.84 ($\pi = 0.5$), but the correlations of ΔAUC with the other two IncV metrics increases with π . When $\pi = 0.01$, ΔAUC and $\Delta sBrS$ are negatively correlated and their correlation -0.11 is the smallest among the three pairs; when $\pi = 0.5$, they are the highest positively correlated. We also show the scatter plots of each pair under different π in Figure S7 (supplementary material).

Concordance. The sign of an IncV metric is often used to decide whether the new model is better than the existing one. Positive IncVs favor the new model, while negative or zero values favor the existing one. Here, we define a concordance measure, which quantifies the consistency of the conclusions reached by a pair of IncV metrics.

Take ΔAP and $\Delta sBrS$ as an example. Under a scenario, we call the pair concordant if both are > 0 or ≤ 0 . If one is > 0 and the other is ≤ 0 , the pair is discordant. The measure of concordance is defined as the proportion of scenarios where the pair is concordant minus the proportion of scenarios where it is discordant. For instance, when $\pi = 0.01$, ΔAP and $\Delta sBrS$ are concordant in about 97% of the total 640 scenarios (i.e., all the combinations of β_1 , β_2 , and β_3 values at each π) and discordant in about 3%. Thus, the concordance measure is 0.93.

Table 1 reports the concordance for all three pairs of the IncV metrics under each π . The results are similar to those above for the Pearson correlation. When π is small, such as 0.01, 0.05, and 0.1, ΔAP and ΔsBrS are the most concordant; when $\pi = 0.2$ or 0.5, ΔAUC and ΔsBrS are the most concordant. ΔAUC and ΔAP are the least concordant for all values of π .

When π is close to 0.5, the three IncV metrics tend to agree. Using any of them, we would very likely reach the same conclusion about whether the new model is better. However, when the event rate is low, i.e., for a rare outcome, ΔAUC can be inconsistent with both ΔsBrS and ΔAP .

4.2.3 ΔAUC versus ΔAP in selected scenarios

Next, we single out four scenarios for an in-depth comparison between ΔAUC and ΔAP at $\pi = 0.01$. The first two scenarios have similar ΔAUC but different ΔAP (Figure 5), whereas the next two have similar ΔAP but different ΔAUC (Figure 6).

Similar ΔAUC but different ΔAP . The two scenarios are (i) $\beta_1 = 1$, $\beta_2 = 0.8$, and $\beta_3 = 0.2$, and (ii) $\beta_1 = 1$, $\beta_2 = 0.8$, and $\beta_3 = -0.5$. In both cases, ΔAUC is around 0.06, but ΔAP is 0.33 for scenario (i) and -0.072 for scenario (ii).

In scenario (i), both the ROC and PR curves of the two-marker model dominate those of the one-marker model, respectively. This indicates that the two-marker model is better at each point, and consequently, $\Delta(\alpha)$ is positive throughout (Figure 5 (c)). In this case, both ΔAUC and ΔAP are positive. However, the size of ΔAP 0.33 is much larger than ΔAUC of 0.06, due to the large weight $w_{\text{AP}}(\alpha)$ at the upper quantiles (Figure 5 (c)).

In scenario (ii), both the two ROC curves and PR curves cross, and $\Delta(\alpha)$ is below zero for upper quantiles and above zero for lower quantiles (Figure 5 (c)). This implies that the two-marker model can better separate between events and non-events for the lower-risk group, but not for the higher-risk group. As a result, ΔAUC and ΔAP are conflicting. ΔAUC is positive because the area under $\Delta(\alpha)$ curve above zero is larger than that below zero. However, ΔAP is negative, as it weights the below-zero $\Delta(\alpha)$ heavily. In such a situation, is the two-marker model better? The answer should be determined by the objective of the study. If this is a classification problem, the new marker indeed improves the discrimination on average. However, if the goal is to screen for the high-risk group, the two-marker model is worse.

Similar ΔAP but Different ΔAUC . The next two scenarios are (iii) $\beta_1 = 0.7$, $\beta_2 = 0.3$, and $\beta_3 = -0.3$, and (iv) $\beta_1 = 0.6$, $\beta_2 = 0.7$, and $\beta_3 = -0.4$. In both cases, ΔAP values are almost 0, but ΔAUC is approximately 0 for scenario (iii) and 0.202 for scenario (iv).

In scenario (iii), the two ROC curves and the two PR curves are almost identical. This indicates that adding the new marker does not change the separation of the distributions of the risk score between events and non-events. It is also reflected in Figure 6 (c) where the entire $\Delta(\alpha)$ curve almost overlaps with the zero line. Thus, both ΔAUC and ΔAP are close to zero. This is an example of both metrics agreeing that the new marker is “useless”.

In scenario (iv), although the two-marker model makes poorer predictions for the higher-risk group, its prediction is significantly better for the rest. Thus, ΔAUC is positive and

sizable. However, since ΔAP weights heavily on the high-risk group, the improvement on the majority is offset by the worse performance at the upper quantiles, which leads to a close-to-zero ΔAP . If the objective is to identify the high-risk group, the new marker is not helpful because it results in a much lower PPV for subjects with high-risk scores.

4.3 What if the two-marker model is the true model, i.e., $\beta_3 = 0$?

Figures S8 and S9 in the supplementary material examine this question and show the scatter plots and plots of the summary statistics of ΔAUC , ΔAP , and $\Delta sBrS$ for different π . As expected, all the IncVs are positive. For a smaller π , ΔAP ranges wider than ΔAUC does. As π increases, these two metrics get closer to each other. When $\pi = 0.5$, $\Delta sBrS$ has the widest range.

Since all the IncVs are positive, their concordance is all 1. Table S1 (supplementary material) lists the Pearson correlation between each pair of the IncV metrics, which are all positive. When π is small, $\Delta sBrS$ is more strongly correlated with ΔAP than with ΔAUC . As π increases, all three IncV metrics are strongly correlated with each other.

5 Discussion

In this article, we focus on two IncV metrics: ΔAUC and ΔAP , for comparing a new risk model with an existing one. We showed that they are intrinsically connected: both can be expressed as a function of $\Delta(\alpha)$, a quantity characterizing the change of the separation of the risk score distributions between events and non-events from an existing risk model to a new one. However, ΔAP emphasizes the change in the higher-risk group, whereas ΔAUC weights the change equally. Because of this difference, they do not always agree with each other. In the numerical study where both working models are misspecified, the correlation between ΔAUC and ΔAP ranges from negative to positive as the event rate π increases from 0.01 to 0.5.

Additionally, ΔAP has a wide range, from negative to positive. However, the size of ΔAUC values is much smaller, subject to the criticisms of it being insensitive (Pepe et al., 2004). ΔAUC is also rarely negative, unable to reflect the situations when the new model is worse than the existing one. These differences in the magnitude between ΔAP and ΔAUC are more evident when the event rate is low. The derived analytical expressions of these two metrics provide a new perspective that explains the insensitivity of ΔAUC . When a new model improves the prediction performance for a subgroup, for example, the high-risk group, the AUC weakens the “local” superior performance by averaging over the entire range. In contrast, the AP augments this “local” improvement by assigning heavier weights.

Likewise, if a study objective concerns the low-risk group, we could consider using the area under a curve of negative predicted values versus specificity ($1 - FPR$) as the accuracy metric. Following our derivation of AP, the IncV in this area should also be a weighted average of the change in the separation of the risk score distributions between events and non-events, and the weight is larger for the lower-tail quantiles of the risk score.

In this article, we also find that ΔAUC and ΔAP have different relationships with the only strictly proper scoring rule $\Delta sBrS$. In general, ΔAP is always strongly positively correlated

with ΔsBrS . On the other hand, as π increases, the correlation between ΔAUC and ΔsBrS changes from negative to positive, similar to the correlation between ΔAUC and ΔAP .

Our paper focuses on situations when neither of the working models is the true model. Under such situations, different IncV metrics likely lead to conflicting conclusions on whether the new model is better than the existing one. Choosing which metric to evaluate the new model depends on the purpose of the risk model. Is it for making a diagnosis, screening for subjects with some disease, or identifying the high-risk subjects that will develop an event? The purpose of the risk model requires that it performs well in one or more areas, such as calibration, discrimination, and identification of the high-risk group. In our data example, the risk models are used to identify the high-risk group that needs counseling for fertility preservation interventions and hormone replacement therapy. This example illustrates a situation that ΔAP is more appropriate whereas ΔAUC could be misleading. However, in other applications such as classification problems, ΔAUC would serve better.

When one of the working models is the true model, Pepe et al. (2013) prove that $H_0 : p(X, Y) = p(X)$ is equivalent to the null hypotheses concerning no improvement in the accuracy measures such as the AUC, net reclassification index (NRI), or integrated discrimination improvement (IDI) (Pencina et al., 2008). This is consistent with the results of our numerical study in which the two-marker model is the true model. In this case, the two ROC or PR curves never cross. However, when both working models are misspecified, the two curves might cross, and thus, the above equivalence among the null hypotheses does not hold.

A good IncV metric should be a proper scoring rule (strictly or semi). Hilden (2014) pointed out that “Under no circumstances should a risk assessor, by some clever systematic distortion of the risk assessments, be able to improve his apparent performance.” That is, the true model should always be the winner or among the winners. Although several IncV parameters such as NRI and IDI has gained popularity, they are not proper scoring rules. Another proper scoring rule is the decision curve and net benefit (NB) (Pepe et al., 2015). We did not include the NB in our analysis. The NB is designed for making treatment decisions given a patient’s risk tolerance, while all three metrics in this paper are about model evaluation. Also, the NB depends on a threshold probability p_t , but the metrics here are threshold-free. As future work, we are interested in comparing ΔAUC , ΔAP , and ΔsBrS with ΔNB .

Because the ranges of AUC, AP, and sBrS are different, the domains of their IncV parameters are also different: $\Delta\text{AUC} \in [-0.5, 0.5]$, $\Delta\text{AP} \in [\pi - 1, 1 - \pi]$, and $\Delta\text{sBrS} \in [-1, 1]$. It may be worthwhile to consider rescaling these IncV metrics to range from -1 and 1 . Alternatively, an IncV metric can be defined as a ratio such as $\Psi_{\text{new}}/\Psi_{\text{old}}$.

As mentioned earlier, the AUC is conditional on the disease status. Thus, it can be estimated from either a prospective cohort study or a case-control study. In contrast, the AP is conditional on the risk score, and consequently, it is previously only possible to be estimated from cohort studies. With the derived expression of the AP in equation (A.5), we provide a potential solution to estimating the AP from a case-control design: one can estimate the AP using (i) an estimated or assumed event rate, and (ii) the risk score distributions of events and non-events estimated from a case-control study.

A Appendix

A.1 Estimation of AUC, AP, and sBrS for binary outcomes

Suppose that the data $\mathfrak{D} = \{(D_i, \mathbf{X}_i), \mathbf{i} = 1, \dots, \mathbf{n}\}$ is collected from n subjects. Let \hat{p}_i denoted the estimated risk, described in Remark 1. Let \hat{r}_i be a risk score, which is a non-decreasing transformation of \hat{p}_i . The AUC and AP are estimated using \hat{r}_i by the following nonparametric estimators

$$\widehat{\text{AUC}} = \frac{\sum_{i=1}^n \sum_{j=1}^n I(D_i = 1)I(D_j = 0)I(\hat{r}_i > \hat{r}_j)}{\sum_{i=1}^n \sum_{j=1}^n I(D_i = 1)I(D_j = 0)},$$

and

$$\widehat{\text{AP}} = \frac{\sum_{i=1}^n \left[I(D_i = 1) \sum_{j=1}^n I(D_j = 1)I(\hat{r}_j > \hat{r}_i) / \sum_{j=1}^n I(\hat{r}_j > \hat{r}_i) \right]}{\sum_{i=1}^n I(D_i = 1)}.$$

The BrS can be estimated using \hat{p}_i by $\widehat{\text{BrS}} = n^{-1} \sum_{i=1}^n (D_i - \hat{p}_i)^2$. The event rate is estimated as $\hat{\pi} = n^{-1} \sum_{i=1}^n D_i$. Then the sBrS is estimated as $\widehat{\text{sBrS}} = 1 - \widehat{\text{BrS}} / [\hat{\pi}(1 - \hat{\pi})]$.

A.2 Derivation of AUC and AP

Let $\pi = Pr(D = 1)$ be the event rate, and $r(\mathbf{X}) = \mathbf{r}_{\mathbf{X}}$ be a risk score. Let $F(c) = Pr(r_{\mathbf{X}} \leq c)$ denote its cumulative distribution function (CDF) for the entire population, and $F_1(c) = Pr(r_{\mathbf{X}} \leq c \mid D = 1)$ and $F_0(c) = Pr(r_{\mathbf{X}} \leq c \mid D = 0)$ denote its CDFs for events and non-events, respectively.

The TPR, FPR, and PPV are

$$\text{TPR}(c) = Pr(r_{\mathbf{X}} > c \mid D = 1) = 1 - F_1(c) \quad (\text{A.1})$$

$$\text{FPR}(c) = Pr(r_{\mathbf{X}} > c \mid D = 0) = 1 - F_0(c) \quad (\text{A.2})$$

$$\begin{aligned} \text{PPV}(c) &= Pr(D = 1 \mid r_{\mathbf{X}} > c) = \frac{Pr(D = 1, r_{\mathbf{X}} > c)}{Pr(r_{\mathbf{X}} > c)} = \frac{\pi [1 - F_1(c)]}{1 - F(c)} \\ &= \frac{\pi [1 - F_1(c)]}{\pi [1 - F_1(c)] + (1 - \pi) [1 - F_0(c)]} \end{aligned} \quad (\text{A.3})$$

where $1 - F(c) = \pi [1 - F_1(c)] + (1 - \pi) [1 - F_0(c)]$.

AUC is the area under the ROC curve, which can be expressed as

$$\text{AUC} = \int_{-\infty}^{\infty} \text{TPR}(c) d\text{FPR}(c) = 1 - \int_{-\infty}^{\infty} \text{FPR}(c) d\text{TPR}(c) = \int_{-\infty}^{\infty} [1 - \text{FPR}(c)] d\text{TPR}(c),$$

because $\int_{-\infty}^{\infty} d\text{TPR}(c) = 1$. Using the expressions in equations (A.1) and (A.2), we have

$$\text{AUC} = \int_{-\infty}^{\infty} F_0(c) d[1 - F_1(c)] = \int_{-\infty}^{\infty} F_0(c) dF_1(c).$$

Let $q_\alpha = F_1^{-1}(\alpha)$ be the α -th quantile of the F_1 distribution, i.e., $F_1(q_\alpha) = \alpha$. Thus, let $c = q_\alpha$, and we have

$$\text{AUC} = \int_0^1 F_0(q_\alpha) d\alpha. \quad (\text{A.4})$$

AP is the area under the PR curve, which can be expressed as

$$\text{AP} = \int_{-\infty}^{\infty} \text{PPV}(c) d\text{TPR}(c).$$

Using the expressions in equations (A.1) and (A.3), we have

$$\begin{aligned} \text{AP} &= \int_{-\infty}^{\infty} \frac{\pi F_1(c)}{\pi F_1(c) + (1-\pi)F_0(c)} d[1 - F_1(c)] \\ &= \int_{-\infty}^{\infty} \frac{\pi [1 - F_1(c)]}{\pi [1 - F_1(c)] + (1-\pi)[1 - F_0(c)]} dF_1(c) \\ &= \int_{-\infty}^{\infty} \left\{ \frac{\pi [1 - F_1(c)] + (1-\pi)[1 - F_0(c)]}{\pi [1 - F_1(c)]} \right\}^{-1} dF_1(c) \\ &= \int_{-\infty}^{\infty} \left\{ 1 + \frac{1-\pi}{\pi} \frac{1 - F_0(c)}{1 - F_1(c)} \right\}^{-1} dF_1(c). \end{aligned}$$

Again, let $c = q_\alpha$, we have

$$\text{AP} = \int_0^1 \left\{ 1 + \frac{\pi^{-1} - 1}{1 - \alpha} [1 - F_0(q_\alpha)] \right\}^{-1} d\alpha. \quad (\text{A.5})$$

A.3 Weight w_{AP} in ΔAP

Let AP_{old} and α_{new} denote the AP of the existing and new models:

$$\begin{aligned} \text{AP}_{old} &= \int_0^1 \left\{ 1 + \frac{\pi^{-1} - 1}{1 - \alpha} [1 - F_{old,0}(q_{old,\alpha})] \right\}^{-1} d\alpha, \\ \text{AP}_{new} &= \int_0^1 \left\{ 1 + \frac{\pi^{-1} - 1}{1 - \alpha} [1 - F_{new,0}(q_{new,\alpha})] \right\}^{-1} d\alpha. \end{aligned}$$

Thus, with arithmetic operations, the IncV in AP can be expressed as

$$\Delta\text{AP} = \text{AP}_{old} - \text{AP}_{new} = \int_0^1 w_{\text{AP}}(\alpha) [F_{new,0}(q_{new,\alpha}) - F_{old,0}(q_{old,\alpha})] d\alpha,$$

where

$$w_{\text{AP}}(\alpha) = \frac{\frac{\pi^{-1} - 1}{1 - \alpha}}{\left[1 + (\pi^{-1} - 1) \frac{1 - F_{new,0}(q_{new,\alpha})}{1 - \alpha} \right] \left[1 + (\pi^{-1} - 1) \frac{1 - F_{old,0}(q_{old,\alpha})}{1 - \alpha} \right]}. \quad (\text{A.6})$$

It is a function of α and π . It also depends on $F_{new,0}(q_{new,\alpha})$ and $F_{old,0}(q_{new,\alpha})$. In general, $F_0(q_\alpha) \geq \alpha$ because the density curve for non-events is to the left of that for events. Thus, how the weight changes with α and π is mainly determined by the numerator $(\pi^{-1} - 1)/(1 - \alpha)$. However, when π and α are fixed, larger values of $F_{old,0}(q_{old,\alpha})$ or $F_{new,0}(q_{new,\alpha})$ or both, i.e., better performance of at least one model, lead to larger weights.

Acknowledgements

The data example is from the St. Jude Lifetime cohort study, supported by National Cancer Institute grant U01CA195547 (PIs Hudson MM and Robinson LL). We thank the St. Jude Lifetime cohort study participants and their families for providing the time and effort for participation and the internet team at St. Jude Children’s Research Hospital for the development of the web application of the risk prediction models.

Funding

Dr. Yuan’s research is supported by the Natural Sciences and Engineering Research Council of Canada (RGPIN-2019-04862).

Abbreviations

AOF: acute ovarian failure

AP: average positive predicted value or average precision

AUC: area under the ROC curve

BrS: Brier score

CDF: cumulative distribution function

FPR: false positive rate

IDI: integrated discrimination improvement

IncV: incremental value

NB: net benefit

NRI: net reclassification index

PPV: positive predicted value

PR: precision-recall

ROC: receiver operating characteristic

sBrS: scaled Brier score

TPR: true positive rate

Availability of data and materials

The R code for the numerical study and analyzing the data example is available in <https://github.com/miche>

Ethics approval and consent to participate

Not applicable.

Competing interests

The authors declare that they have no competing interests.

Authors' contributions

QZ and YY developed the concept, designed the analytical and numerical studies and drafted the manuscript. LZ conducted the numerical study and analyzed the data example. RB and MH prepared the data from the St. Jude Lifetime cohort Study. LZ, RB, and MH revised the manuscript. All the authors read and approved the final manuscript.

References

- Badawi, O., Liu, X., Hassan, E., Amelung, P. J., and Swami, S. (2018). Evaluation of icu risk models adapted for use as continuous markers of severity of illness throughout the icu stay. *Critical care medicine*, 46(3):361–367.
- Buckley, D. I., Fu, R., Freeman, M., Rogers, K., and Helfand, M. (2009). C-reactive protein as a risk factor for coronary heart disease: a systematic review and meta-analyses for the us preventive services task force. *Annals of internal medicine*, 151(7):483–495.
- Chaudhury, S., Brookes, K. J., Patel, T., Fallows, A., Guetta-Baranes, T., Turton, J. C., Guerreiro, R., Bras, J., Hardy, J., Francis, P. T., et al. (2019). Alzheimer’s disease polygenic risk score as a predictor of conversion from mild-cognitive impairment. *Translational psychiatry*, 9(1):1–7.
- Clark, R. A., Mostoufi-Moab, S., Yasui, Y., Vu, N. K., Sklar, C. A., Motan, T., Brooke, R. J., Gibson, T. M., Oeffinger, K. C., Howell, R. M., Smith, S. A., Lu, Z., Robison, L. L., Chemaitilly, W., Hudson, M. M., Armstrong, G. T., Nathan, P. C., and Yuan, Y. (2020). Predicting acute ovarian failure in female survivors of childhood cancer: a cohort study in the childhood cancer survivor study (ccss) and the st jude lifetime cohort (sjlife). *The Lancet Oncology*, 21(3):436–445.
- Cook, N. R., Buring, J. E., and Ridker, P. M. (2006). The effect of including c-reactive protein in cardiovascular risk prediction models for women. *Annals of internal medicine*, 145(1):21–29.
- Cox, D. R. et al. (1972). Regression models and life tables. *JR stat soc B*, 34(2):187–220.
- Elliott, J., Bodinier, B., Bond, T. A., Chadeau-Hyam, M., Evangelou, E., Moons, K. G., Dehghan, A., Muller, D. C., Elliott, P., and Tzoulaki, I. (2020). Predictive accuracy of a polygenic risk score-enhanced prediction model vs a clinical risk score for coronary artery disease. *Jama*, 323(7):636–645.
- Howell, R. M., Smith, S. A., Weathers, R. E., Kry, S. F., and Stovall, M. (2019). Adaptations to a generalized radiation dose reconstruction methodology for use in epidemiologic studies: an update from the md anderson late effect group. *Radiation research*, 192(2):169–188.

- Hudson, M. M., Ness, K. K., Nolan, V. G., Armstrong, G. T., Green, D. M., Morris, E. B., Spunt, S. L., Metzger, M. L., Krull, K. R., Klosky, J. L., et al. (2011). Prospective medical assessment of adults surviving childhood cancer: study design, cohort characteristics, and feasibility of the st. jude lifetime cohort study. *Pediatric blood & cancer*, 56(5):825–836.
- Kattan, M. W. and Gerds, T. A. (2018). The index of prediction accuracy: an intuitive measure useful for evaluating risk prediction models. *Diagnostic and prognostic research*, 2(1):7.
- Manning, C. D. and Schütze, H. (1999). *Foundations of statistical natural language processing*. MIT Press, USA.
- Mosley, J. D., Gupta, D. K., Tan, J., Yao, J., Wells, Q. S., Shaffer, C. M., Kundu, S., Robinson-Cohen, C., Psaty, B. M., Rich, S. S., et al. (2020). Predictive accuracy of a polygenic risk score compared with a clinical risk score for incident coronary heart disease. *Jama*, 323(7):627–635.
- Pencina, M. J., D’Agostino Sr, R. B., D’Agostino Jr, R. B., and Vasan, R. S. (2008). Evaluating the added predictive ability of a new marker: from area under the roc curve to reclassification and beyond. *Statistics in medicine*, 27(2):157–172.
- Pepe, M. S. (2003). *The statistical evaluation of medical tests for classification and prediction*. Oxford University Press, Oxford.
- Pepe, M. S., Fan, J., Feng, Z., Gerds, T., and Hilden, J. (2015). The net reclassification index (nri): a misleading measure of prediction improvement even with independent test data sets. *Statistics in biosciences*, 7(2):282–295.
- Pepe, M. S., Janes, H., Longton, G., Leisenring, W., and Newcomb, P. (2004). Limitations of the odds ratio in gauging the performance of a diagnostic, prognostic, or screening marker. *American journal of epidemiology*, 159(9):882–890.
- Pepe, M. S., Kerr, K. F., Longton, G., and Wang, Z. (2013). Testing for improvement in prediction model performance. *Statistics in medicine*, 32(9):1467–1482.
- Raghavan, V., Bollmann, P., and Jung, G. S. (1989). A critical investigation of recall and precision as measures of retrieval system performance. *ACM Transactions on Information Systems (TOIS)*, 7(3):205–229.
- Steyerberg, E. W., Vickers, A. J., Cook, N. R., Gerds, T., Gonen, M., Obuchowski, N., Pencina, M. J., and Kattan, M. W. (2010). Assessing the performance of prediction models: a framework for some traditional and novel measures. *Epidemiology (Cambridge, Mass.)*, 21(1):128.
- Su, W., Yuan, Y., and Zhu, M. (2015). A relationship between the average precision and the area under the roc curve. In *Proceedings of the 2015 International Conference on The Theory of Information Retrieval*, pages 349–352. ACM.

- Tang, M., Hu, P., Wang, C.-F., Yu, C.-Q., Sheng, J., and Ma, S.-J. (2019). Prediction model of cardiac risk for dental extraction in elderly patients with cardiovascular diseases. *Gerontology*, 65(6):591–598.
- Uno, H., Cai, T., Tian, L., and Wei, L. (2007). Evaluating prediction rules for t-year survivors with censored regression models. *Journal of the American Statistical Association*, 102:527–537.
- Xiao, J., Ding, R., Xu, X., Guan, H., Feng, X., Sun, T., Zhu, S., and Ye, Z. (2019). Comparison and development of machine learning tools in the prediction of chronic kidney disease progression. *Journal of translational medicine*, 17(1):119.
- Yuan, Y., Su, W., and Zhu, M. (2015). Threshold-free measures for assessing the performance of medical screening tests. *Frontiers in Public Health*, 3:57.
- Yuan, Y., Zhou, Q. M., Li, B., Cai, H., Chow, E. J., and Armstrong, G. T. (2018). A threshold-free summary index of prediction accuracy for censored time to event data. *Statistics in medicine*, 37(10):1671–1681.
- Zweig, M. H. and Campbell, G. (1993). Receiver-operating characteristic (roc) plots: a fundamental evaluation tool in clinical medicine. *Clinical chemistry*, 39(4):561–577.

Table 1: Pearson correlation and concordance measure of each pair of the IncV metrics for different event rates π .

Pearson Correlation					
Comparison	$\pi = 0.01$	$\pi = 0.05$	$\pi = 0.1$	$\pi = 0.2$	$\pi = 0.5$
$\Delta sBrS$ vs ΔAP	0.995	0.992	0.986	0.971	0.837
$\Delta sBrS$ vs ΔAUC	-0.111	0.262	0.479	0.718	0.932
ΔAUC vs ΔAP	-0.086	0.296	0.505	0.708	0.888

Concordance					
Comparison	$\pi = 0.01$	$\pi = 0.05$	$\pi = 0.1$	$\pi = 0.2$	$\pi = 0.5$
$\Delta sBrS$ vs ΔAP	0.931	0.922	0.897	0.856	0.922
$\Delta sBrS$ vs ΔAUC	0.659	0.750	0.828	0.928	1.000
ΔAUC vs ΔAP	0.591	0.672	0.725	0.784	0.922

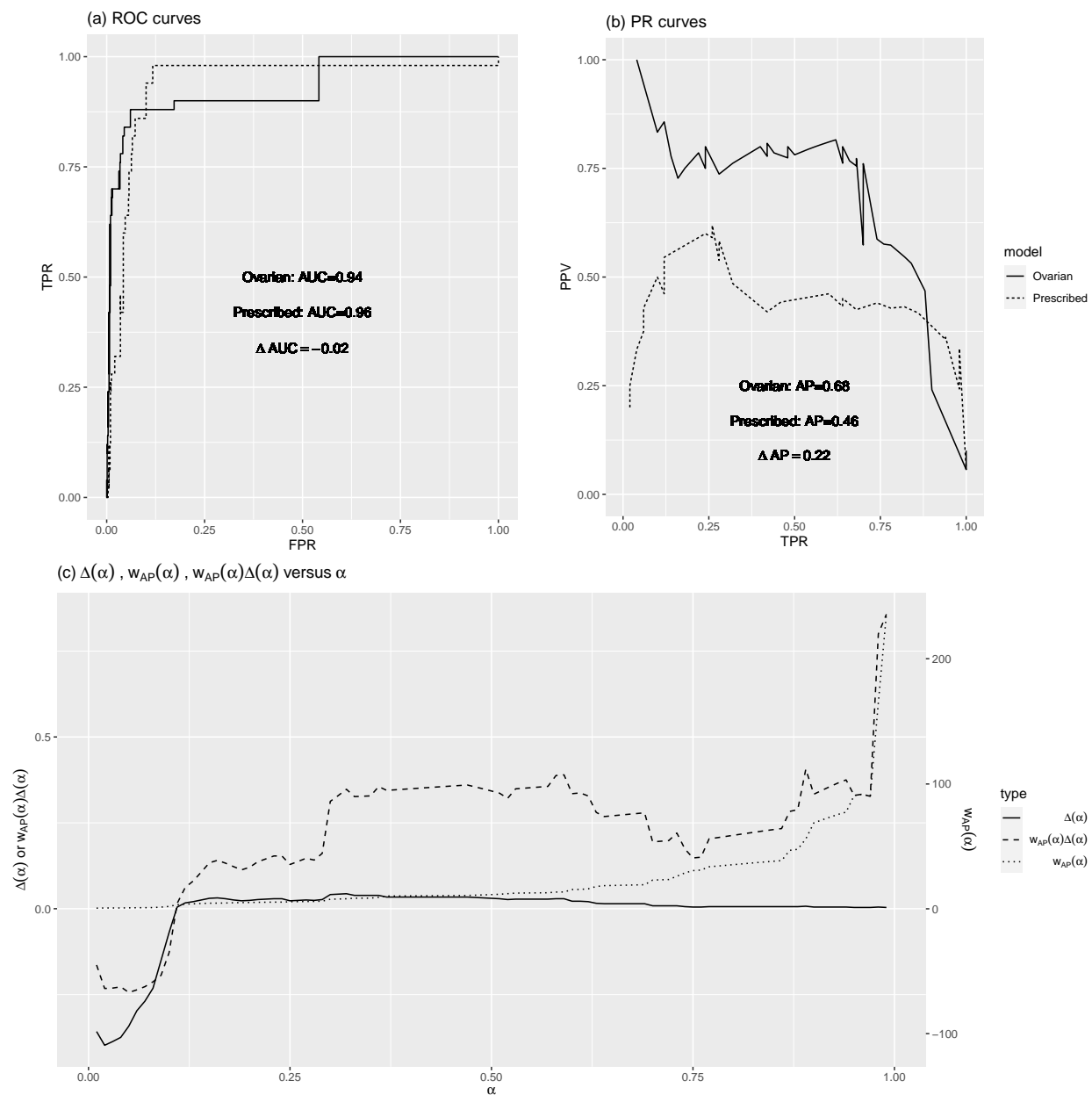


Figure 1: Data example: ovarian-dose vs prescribed-dose.

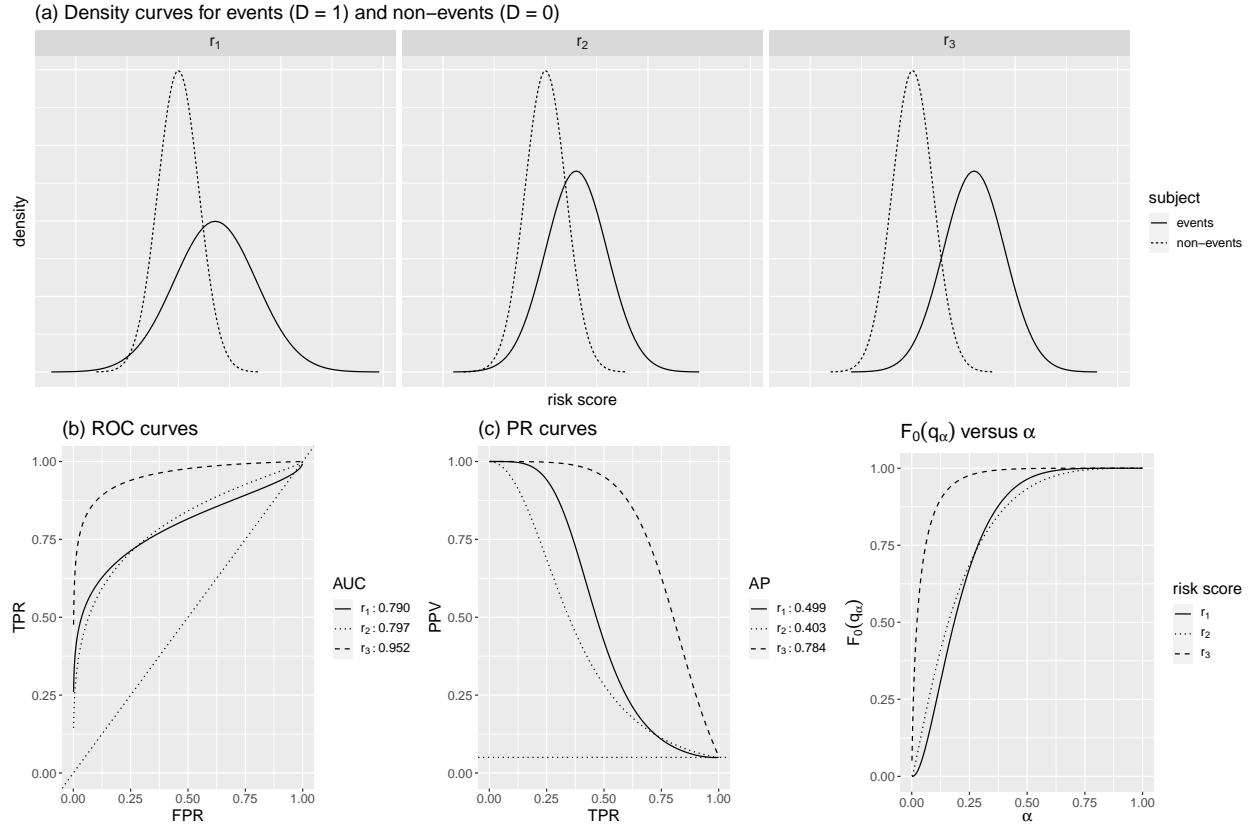


Figure 2: Comparison of three hypothetical risk scores r_1 , r_2 , and r_3 at event rate $\pi = 0.05$.

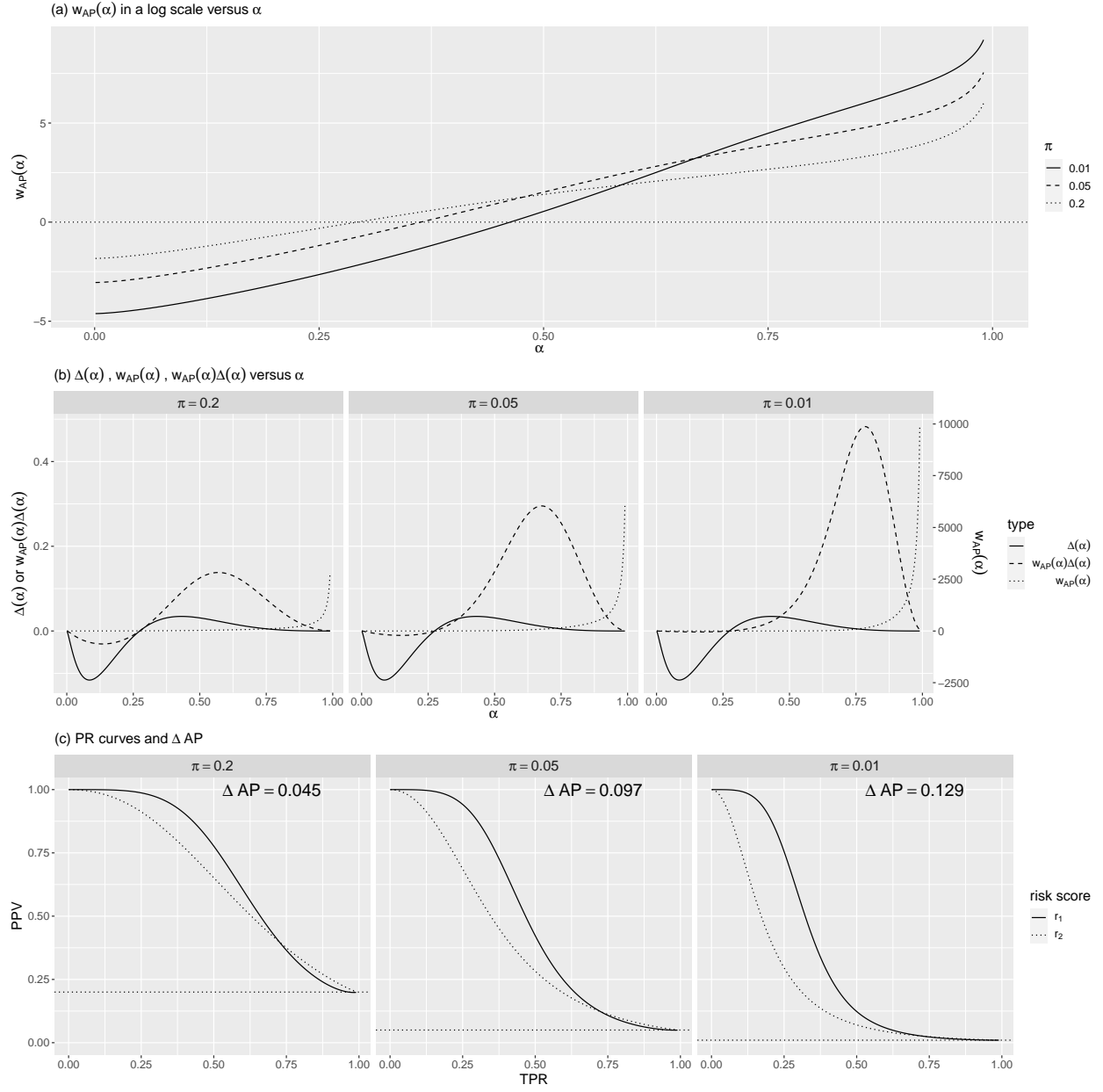


Figure 3: Comparison of hypothetical risk scores r_1 and r_2 under event rates $\pi = 0.2, 0.05, 0.01$.

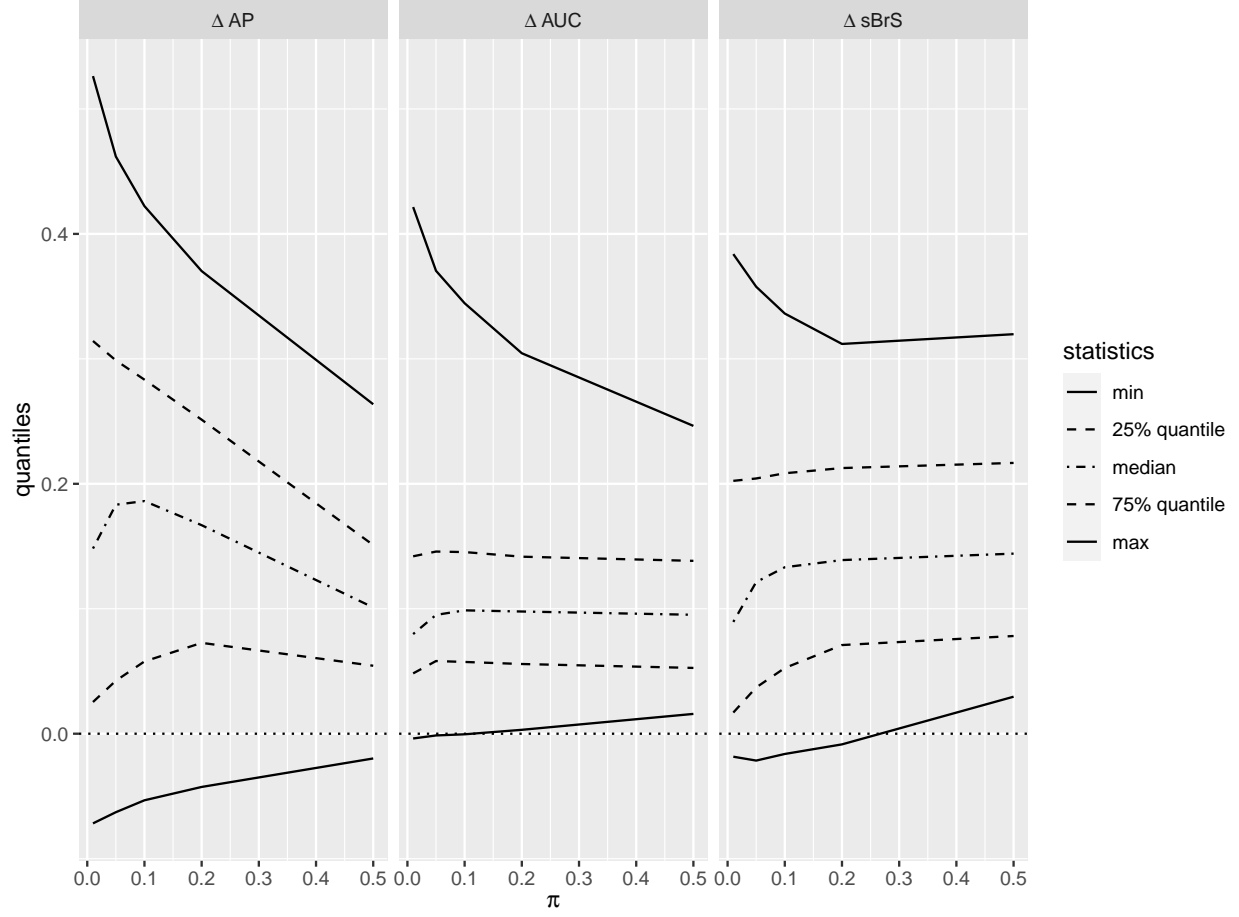


Figure 4: Summary statistics of ΔAUC , ΔAP , and $\Delta sBrS$ versus different event rates π .

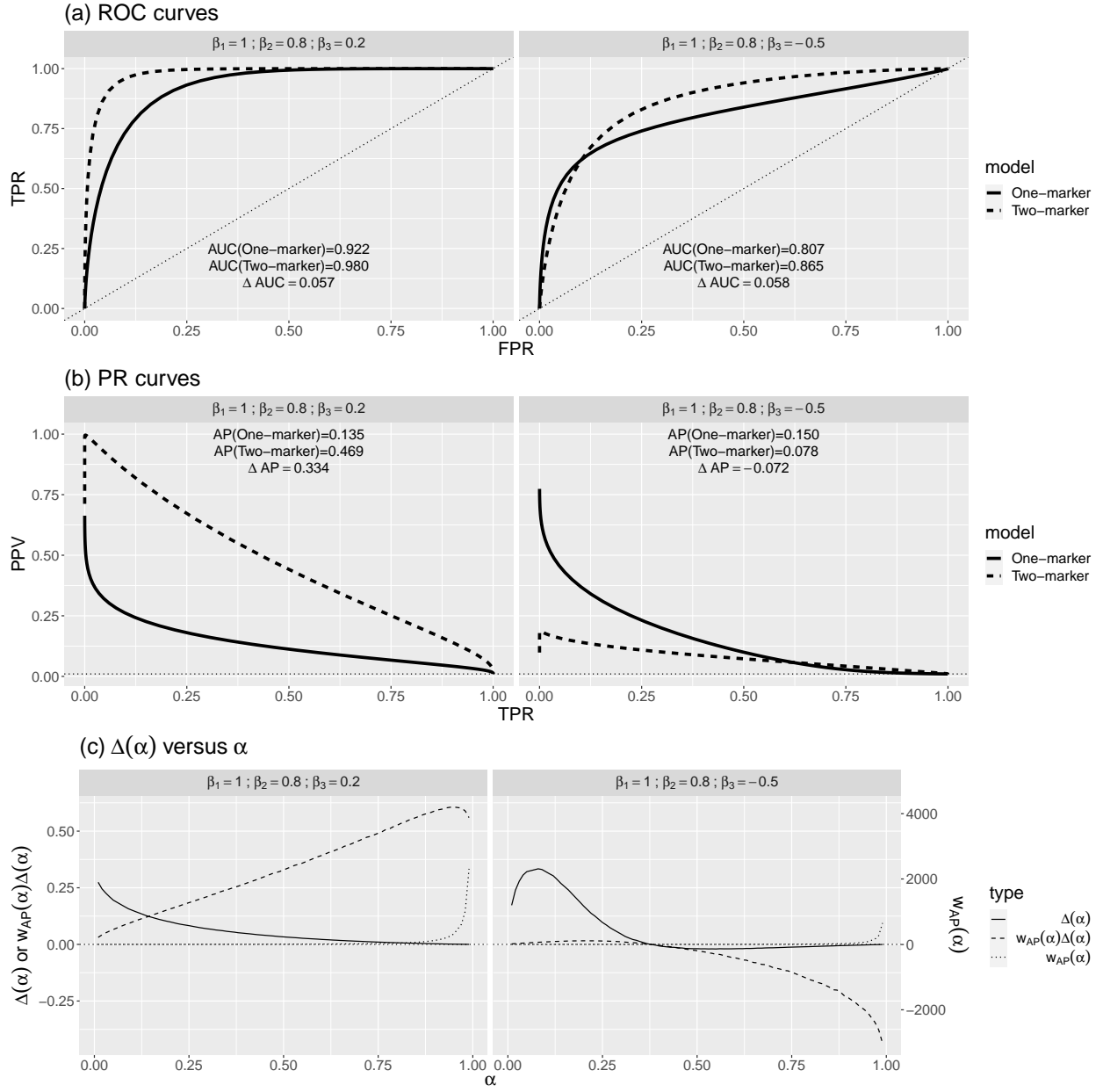


Figure 5: Comparison of two scenarios at event rate $\pi = 0.01$: similar ΔAUC but different ΔAP .

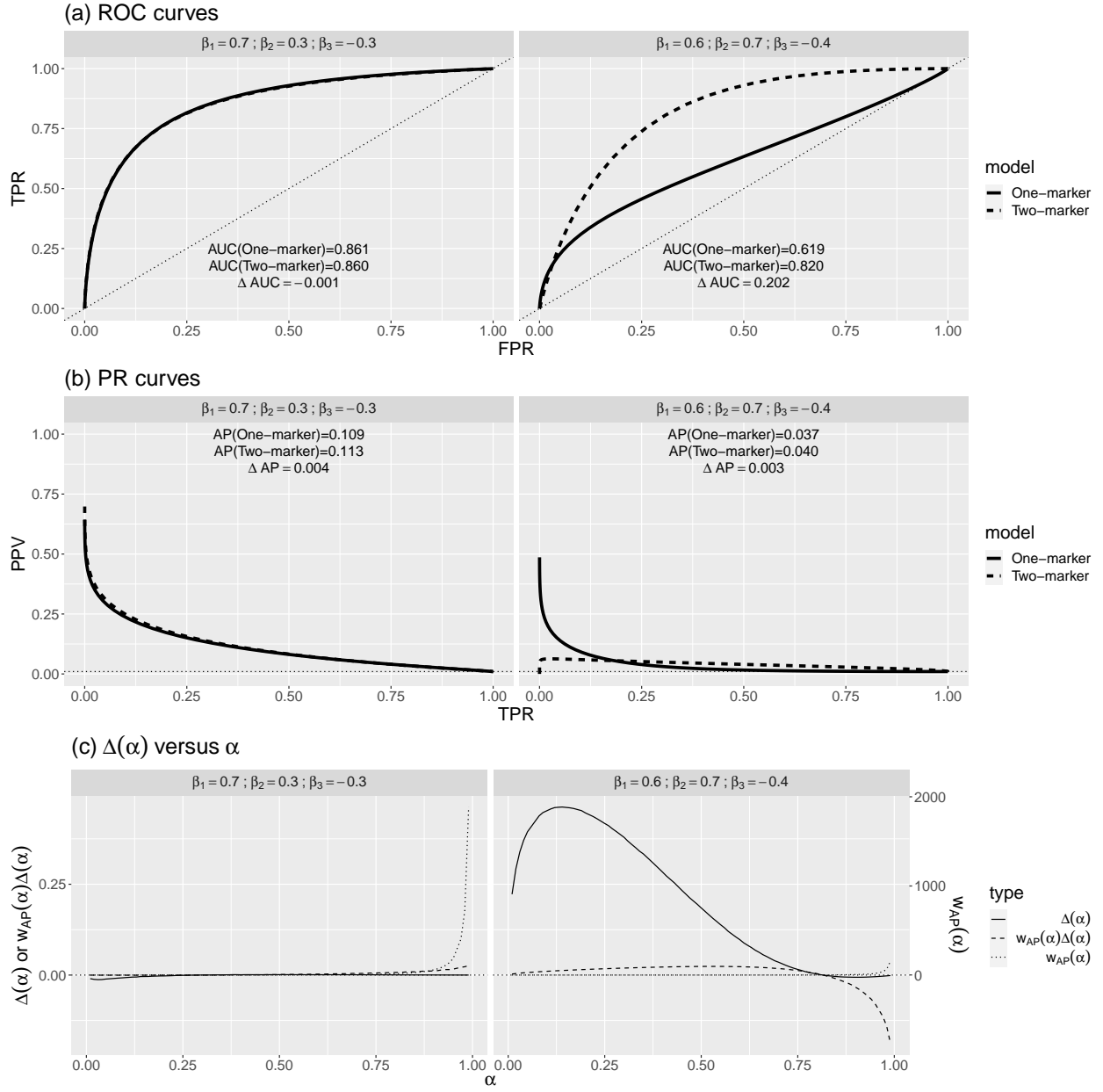


Figure 6: Comparison of two scenarios at event rate $\pi = 0.01$: similar ΔAP but different ΔAUC .

Additional Files

Supplementary material

The supplementary material includes (i) the histograms of the predicted AOF risk obtained from the prescribed-dose model and ovarian-dose model for individuals with and without AOF, respectively, (ii) the procedure of obtaining the IncV parameters under the distributional assumptions of the numerical study, (iii) the results of the numerical study scenarios in which neither of the working risk models is the true model, including plots of the values of each IncV metric for all the scenarios under different event rates, and the scatter plots of each pair of the IncV metrics, and (iv) the results for the scenarios where the two-marker model is the true model, including plots of the values of each IncV metric for all the scenarios under different event rates, plots of their summary statistics, and a table listing the Pearson correlation of each pair of the IncV metrics. (PDF file)